


Fold analysis of crumpled sheets using microcomputed tomography

Yumino Hayase


Department of Physics, Kyushu University, Fukuoka 819-0395, Japan

Hitoshi Aonuma 

Research Institute for Electronic Science, Hokkaido University, Sapporo 060-0812, Japan

Satoshi Takahara 

Graduate School of Information Science and Technology, Hokkaido University, Sapporo 060-0812, Japan

Takahiro Sakaue 

Department of Physical Sciences, Aoyama Gakuin University, 5-10-1 Fuchinobe, Chuo-ku, Sagami-hara, Kanagawa 252-5258, Japan

Shun'ichi Kaneko 

Kazusa DNA Research Institute, 2-6-7 Kazusa-kamatari, Kisarazu, Chiba 292-0818, Japan

Hiizu Nakanishi

Department of Physics, Kyushu University, Fukuoka 819-0395, Japan



(Received 29 April 2021; revised 15 July 2021; accepted 28 July 2021; published 12 August 2021)

Hand-crumpled paper balls involve intricate structure with a network of creases and vertices, yet show simple scaling properties, which suggests self-similarity of the structure. We investigate the internal structure of crumpled papers by the microcomputed tomography (micro-CT) without destroying or unfolding them. From the reconstructed three-dimensional (3D) data, we examine several power laws for the crumpled square sheets of paper of the sizes $L = 50\text{--}300$ mm and obtain the mass fractal dimension $D_M = 2.7 \pm 0.1$ by the relation between the mass and the radius of gyration of the balls and the fractal dimension $2.5 \lesssim d_f \lesssim 2.8$ for the internal structure of each crumpled paper ball by the box counting method in the real space and the structure factors in the Fourier space. The data for the paper sheets are consistent with $D_M = d_f$, suggesting that the self-similarity in the structure of each crumpled ball gives rise to the similarity among the balls with different sizes. We also examine the cellophane sheets and the aluminium foils of the size $L = 200$ mm and obtain $2.6 \lesssim d_f \lesssim 2.8$ for both of them. The micro-CT also allows us to reconstruct 3D structure of a line drawn on the crumpled sheets of paper. The Hurst exponent for the root-mean-square displacement along the line is estimated as $H \approx 0.9$ for the length scale shorter than the scale of the radius of gyration, beyond which the line structure becomes more random with $H \sim 0.5$.

DOI: [10.1103/PhysRevE.104.025005](https://doi.org/10.1103/PhysRevE.104.025005)

I. INTRODUCTION

Crumpling a sheet of paper is the easiest way to make effective shock absorbing buffer. A hand-crumpled paper ball is very light, with typically more than 80% of its volume being empty, and still shows strong resistance against compression. These properties make it ideal spacer for box packing. The origin of these properties is the large stretching energy in comparison with the bending energy for a thin paper sheet. As a result, on crumpling a sheet, Gaussian curvature remains close to zero everywhere except for at singular points of developable cone structures [1–4]. This imposes stringent constraint on the way the paper sheet crumples, thus producing strong resistance against compression even if much of the space is still empty [5,6].

In spite of their complex structure, the balls of crumpled sheet have been known to show simple scaling laws [7–9].

The radius of the ball R follows the scaling relation with the size of the original sheet L as

$$R \sim L^\alpha, \quad (1)$$

and with the force F applied to make the crumpled ball as

$$R \sim F^{-\delta}. \quad (2)$$

The exponents have been estimated as $0.80 \lesssim \alpha \lesssim 0.95$ for aluminium foil and paper, and $\delta \approx 0.2$ for aluminium foil [5–11]. The small value of δ corresponds to the fact that the crumpled sheets resists strongly against compression.

These two power-law relations suggest the fractal structure in the object and may be combined into the single relation [5,12]

$$\frac{R}{h} \propto \left(\frac{L}{h}\right)^\alpha \left(\frac{F}{Yh}\right)^{-\delta}, \quad (3)$$

TABLE I. Sample specifications.

	Tracing paper	Cellophane	Aluminium foil
Manufacturer	Kokuyo Co., Ltd.	Toyo Co.	Shimajima Co., Ltd.
Thickness (mm)	0.0385±0.0008	0.0203±0.0002	0.0115±0.0004
Density (g/m ²)	42.7±0.5	30.0±0.7	27.4±0.6

where Y and h are the two-dimensional (2D) Young modulus and the sheet thickness, respectively. The scaling relations (1) and (2), however, represent different aspects of the structure, namely the former implies the scaling in the structure among the crumpled balls with different sizes, and the latter suggests self-similarity of internal structure of each crumpled ball [13,14].

The internal structure of the crumpled paper ball has been studied by examining the crease networks on unfolded sheets [15–18], the cross sections obtained by cutting the balls in half [11,18,19], or the sequences of holes made by a needle piercing through the balls [13] as well as numerical simulations [12,20–22]. These are indirect way of observing the internal structure.

The x-ray microcomputed tomography (micro-CT) is computer tomography with the high resolution of the order of 100 μm and makes it possible to study the internal structure of crumpled sheets without either unfolding or destroying them. It has been used to study the crumpled balls of aluminium foil to examine the density distribution, the curvatures of the sheets, and the fractal dimensions of the structure [23–25]. In this paper, we use micro-CT to examine the internal structure of crumpled sheets of paper, cellophane, and aluminium foils to determine scaling properties of the structure. Experimental procedure is described in Sec. II, the scaling analysis for the observed quantities is provided in Sec. III, experimental results are presented to obtain several exponents in Sec. IV, and the discussions are given in Sec. V.

II. EXPERIMENTAL PROCEDURE

Square sheets of tracing paper with the side length $L = 50, 100, 200,$ and 300 mm are hand crumpled without any specific protocol. Before being scanned, the crumpled balls are left for 7 days under the environment with the temperature $25 \pm 2^\circ\text{C}$ and the humidity $25 \pm 5\%$ to allow them to settle in order to avoid structure relaxation during about 30 min of the scanning time [26]. The x-ray micro-CT (inspeXio SMX-100CT, Shimadzu Corporation, Kyoto, Japan) is operated at 40 kV with 100 μA and scans a cubic region of the space with the linear size around 4 cm at a resolution $\sim 50\text{--}150$ μm with around 400^3 voxels. We also scan hand crumpled cellophane sheets and aluminium foils of the size $L = 200$ mm following the same procedure described above except that, in the case of aluminium foil, the samples are scanned on the day when they are crumpled. The thicknesses and densities of the samples are listed in Table I.

The micro-CT produces grayscale data for each slice of cross section; the black and white binary data are generated by setting appropriate threshold, and then the 3D structures are reconstructed. Figure 1 shows examples of the reconstructed

3D structures from the CT images and the cross sections for crumpled paper, cellophane sheet, and aluminium foil.

We also reconstruct the 3D configurations of a line drawn on a crumpled paper (Fig. 2). A straight line is drawn using the ink that contains tungsten (Macky gold, Zebra, Tokyo, Japan), which absorbs x rays more efficiently than the paper. Thus the line positions can be extracted from the CT images by setting a higher threshold than that for the paper structure.

III. OBSERVED QUANTITIES AND SCALING ANALYSIS

Before we show our experimental results, we give some scaling analysis for the physical quantities we observe.

a. Three-dimensional structure of crumpled sheets: The mass fractal dimension D_M is defined by the scaling relation between the mass of the paper M and the radius of the crumpled paper ball R as

$$M \sim R^{D_M}. \quad (4)$$

Since the mass of the paper M is proportional to its area, $M \propto L^2$, the mass fractal dimension D_M is related to the exponent α in Eq. (1) as

$$D_M = 2/\alpha. \quad (5)$$

On the other hand, the fractal dimension d_f of the internal structure of each crumpled ball is measured by the box counting method, using the relation

$$N_{\text{box}} \sim l^{-d_f}, \quad (6)$$

where N_{box} is the number of occupied boxes with the linear size l .

These two exponents correspond to two distinct features, i.e., the fractal dimension d_f defined by Eq. (6) describes the self-similarity of each crumpled paper ball structure while the mass fractal dimension D_M represents the similarity among crumpled paper balls with different size L . However, the self-similar structure of each crumpled paper ball suggests the self-similarity among those of different sizes, and Eq. (6) could be extended as

$$N_{\text{box}} \sim \frac{M}{h^2\sigma} \left(\frac{l}{h}\right)^{-d_f}, \quad (7)$$

where h is the paper thickness and σ is the area density of the sheet. This leads to $d_f = D_M$ if R is identified as the box size l that corresponds to $N_{\text{box}} = 1$, i.e.,

$$1 \sim \frac{M}{h^2\sigma} \left(\frac{R}{h}\right)^{-d_f}. \quad (8)$$

The structure factor $S(\mathbf{q})$ is the Fourier transform of the density correlation function $g(\mathbf{r})$,

$$S(\mathbf{q}) = \iiint e^{-i\mathbf{q}\cdot\mathbf{r}} g(\mathbf{r}) d\mathbf{r}, \quad (9)$$

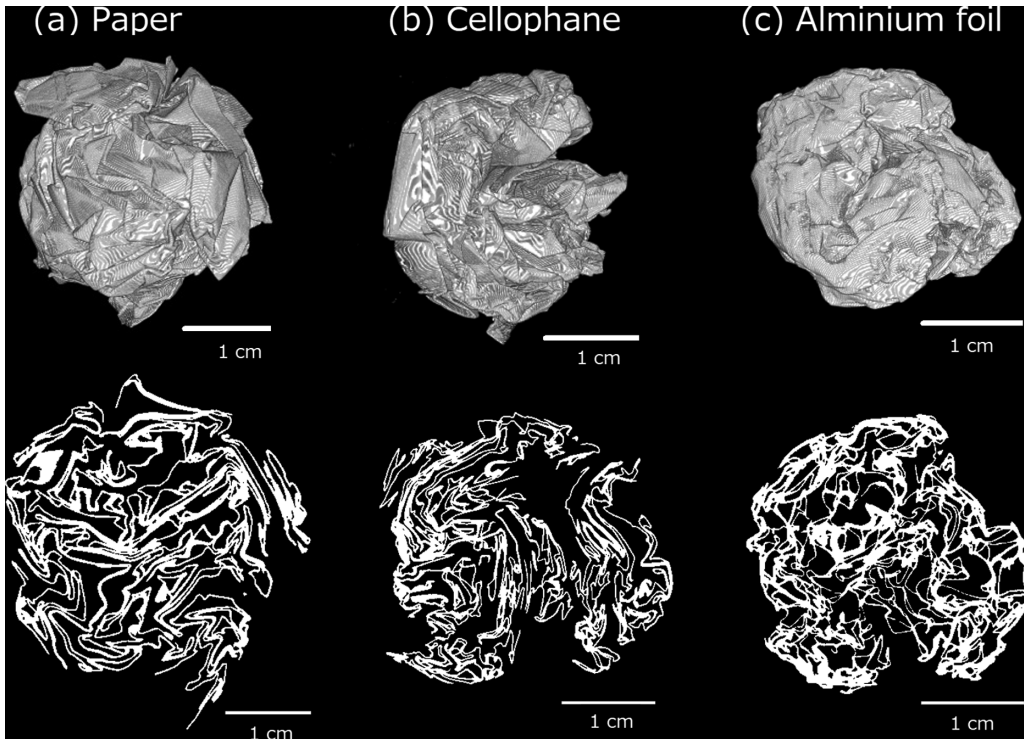


FIG. 1. CT images of crumpled paper (a), cellophane sheet (b), and aluminium foil (c). The upper images are reconstructed 3D structures and the lower images are their cross sections.

where the density correlation is defined by

$$g(\mathbf{r}) = \iiint \langle \rho(\mathbf{r}' + \mathbf{r})\rho(\mathbf{r}') \rangle d\mathbf{r}' \quad (10)$$

in terms of the density distribution $\rho(\mathbf{r})$. Here, $\langle \dots \rangle$ means the ensemble average. If the structures of the crumpled paper ball are self-similar with the fractal dimension d_f , then the density correlation should be of the scaling form,

$$g(r) \sim r^{d_f-3}, \quad (11)$$

then the structure factor is expected to be of the scaling form

$$S(q) \sim q^{-d_f}. \quad (12)$$

b. Cross section of a crumpled sheet: A 3D CT image consists of hundreds of two-dimensional slices of the density

distribution in the cross sections. We analyze the structure of the cross section which contains the center of mass of the crumpled sheet. Suppose that we take the center of mass of the crumpled sheet as the origin of the coordinate and consider the cross section by the $z = 0$ plane. Let $\sigma_{cs}(\mathbf{r}_\perp)$ denote the 2D density distribution on the cross section as a function of a position $\mathbf{r}_\perp = (x, y)$ on the $z = 0$ plane,

$$\sigma_{cs}(\mathbf{r}_\perp) = \int_{-h/2}^{h/2} \rho(\mathbf{r}_\perp, z) dz. \quad (13)$$

The density correlation on the cross section $g_{cs}(\mathbf{r}_\perp)$ is defined by

$$g_{cs}(\mathbf{r}_\perp) = \iint \langle \sigma_{cs}(\mathbf{r}'_\perp + \mathbf{r}_\perp)\sigma_{cs}(\mathbf{r}'_\perp) \rangle d\mathbf{r}'_\perp, \quad (14)$$

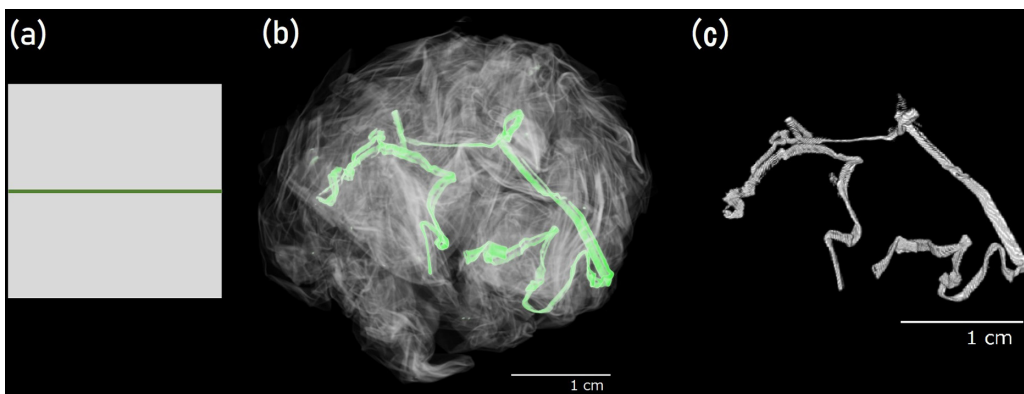


FIG. 2. A line on a crumpled paper of the size $L = 200$ mm. (a) Schematic illustration of a line drawn on a paper with the ink that contains tungsten, (b) an example of three-dimensional image of a crumpled paper with the line, and (c) the extracted 3D image of the line.

and the structure factor of the cross section $S_{cs}(\mathbf{q}_\perp)$ is given by the 2D Fourier transform

$$S_{cs}(\mathbf{q}_\perp) = \iint e^{-i\mathbf{q}_\perp \cdot \mathbf{r}_\perp} g_{cs}(\mathbf{r}_\perp) d\mathbf{r}_\perp, \quad (15)$$

where \mathbf{q}_\perp is the wave vector within the cross-section plane. If we assume the same form as Eq. (11) for g_{cs} as

$$g_{cs}(\mathbf{r}_\perp) \sim r_\perp^{d_f-3}, \quad (16)$$

then the structure factor would behave as

$$S_{cs}(q_\perp) \sim q_\perp^{-(d_f-1)}, \quad (17)$$

which simply shows that the fractal dimension for the cross section is $d_f - 1$.

c. Straight line drawn on a crumpled paper: The CT technique allows us to study the structure of a line drawn on a crumpled paper. A straight line on a flat paper is deformed into a random structure as the paper is crumpled. The configuration of the crumpled line can be represented by the function

$$\mathbf{r}_{\text{line}}(s); \quad 0 \leq s \leq L, \quad (18)$$

where s is the distance along the line from one of the end. The root-mean-square (rms) distance $R_{\text{line}}(s)$ from one of the end points is defined by

$$R_{\text{line}}(s) \equiv \sqrt{\langle [\mathbf{r}_{\text{line}}(s) - \mathbf{r}_{\text{line}}(0)]^2 \rangle}. \quad (19)$$

If this shows the power-law behavior with the Hurst exponent H ,

$$R_{\text{line}}(s) \sim s^H, \quad (20)$$

then the scaling argument based on the self-similarity assumption leads to the scaling law

$$g_{\text{line}}(r) \sim r^{-3+1/H} \quad (21)$$

for the correlation of the line in 3D space, and the scaling law

$$S_{\text{line}}(q) \sim q^{-1/H} \quad (22)$$

for the 3D structure factor of the line.

The size of the crumpled line R_{line} is expected to scale with the size of the paper L as

$$R_{\text{line}} \sim L^{\alpha_{\text{line}}}. \quad (23)$$

If the size of the line R_{line} should be of the same order with the size of the crumpled ball R , and also with rms of the end-to-end distance of the line $R_{\text{line}}(L)$ of Eq. (20), then the Hurst exponent should be related to the mass fractal dimension as

$$H = \alpha_{\text{line}} = \alpha = 2/D_M. \quad (24)$$

IV. EXPERIMENTAL RESULTS

We analyze the 3D structures of the crumpled sheet balls, the cross sections of the balls, and the lines drawn on the paper.

a. Three-dimensional structure of crumpled sheets: Figure 3(a) shows the averaged density distribution of crumpled paper as a function of the distance from the center of mass r . Each line represents the average distribution over the direction and around 10 samples, and the arrows show the average values of the radii of gyration for the corresponding

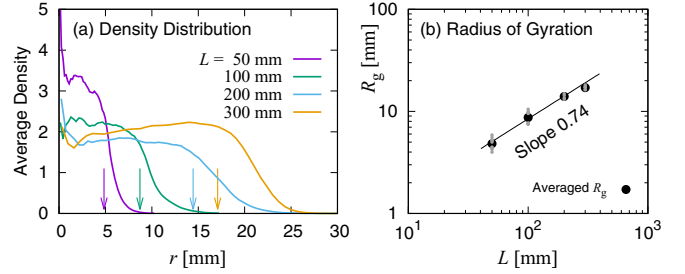


FIG. 3. Density distributions (a) and radii of gyration (b) for crumpled paper sheets of the size $L = 50, 100, 200,$ and 300 mm. (a) Each curve represents average over around 10 samples and the arrows show the average values of the radii of gyration. The density distributions are normalized so that the total mass should be proportional to L^2 . (b) The gray circles and the black circles represent the radius of gyration for each sample and average values over them, respectively.

sizes of the paper. One can see that the averaged density distribution inside the ball is roughly uniform, but it is a slightly decreasing function of r for the crumpled balls of the smaller sheets $L = 50$ and 100 mm, almost constant in the range of $r \lesssim 12$ mm for that of $L = 200$ mm, and slightly increasing in $r \lesssim 16$ mm for that of $L = 300$ mm. It is not clear how this tendency extends to larger sheets. In Fig. 3(b), the radii of gyration R_g are plotted against the paper size L in the logarithmic scale. The data range is less than one decade and not enough to give a precise value of the exponent, but the plots are consistent with the power-law behavior

$$R_g \sim L^\alpha \quad (25)$$

with the exponent $\alpha \approx 0.74$. This gives $D_M = 2/\alpha \approx 2.7$ from Eq. (5).

We estimate the fractal dimensions d_f by the box counting method; the number of occupied boxes N_{box} are plotted against the linear size l_{box} of the box divided by R_g in the logarithmic scale in Figs. 4(a) for paper and 4(b) for cellophane and aluminium foil. Each data point is an average of about 10 samples. The data for different size L or different materials are shifted vertically by multiplying by the factor 2 to avoid overlapping of the plots. The estimated d_f for the crumpled paper is 2.7 from Fig. 4(a). This is consistent with D_M estimated by R_g , and suggests the self-similarity in the 3D structure of the crumpled paper ball as we have discussed. The fractal dimensions d_f for both the cellophane sheet and aluminium foil are estimated as 2.8 from Fig. 4(b).

The structure factors $S(q)$ for the reconstructed 3D structures from the CT data are plotted in the logarithmic scale for the paper of sizes $L = 50$ – 300 mm in Fig. 4(c), and for the paper sheets, the cellophane sheets, and the aluminium foils of the size $L = 200$ mm in Fig. 4(d). Each data point represents averaged value of about 10 samples. These structure factors $S(q)$ show the power-law behavior

$$S(q) \sim q^{-\beta}. \quad (26)$$

The apparent value of the exponent β for the crumpled paper in Fig. 4(c) increases with the paper size L and the fitted value for the largest paper size $L = 300$ mm is $\beta \approx 2.5$. The exponents β for the cellophane sheets and the

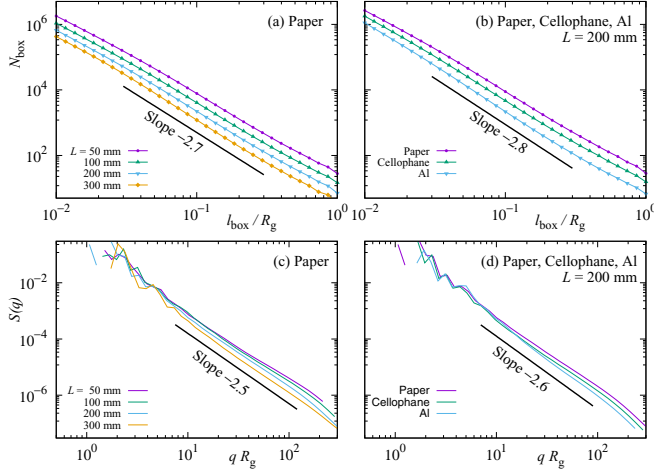


FIG. 4. The box counting data and the averaged structure factors $S(q)$ for the 3D structures of crumpled paper, cellophane, and aluminium foil. The box size l_{box} and the wave number q are scaled by the radii of gyration of each structure. N_{box} for different size L (a) and different materials (b) are shifted by the factor 2 to avoid overlapping.

aluminium foils are estimated from the plots for $L = 200$ mm in Fig. 4(d) as $\beta \approx 2.6$. These values of β estimated by $S(q)$ are slightly smaller than those of d_f estimated by the box counting method although they should coincide as

$$\beta = d_f \quad (27)$$

from Eq. (12) if the self-similarity holds.

b. Cross-section structure of crumpled sheets: The structure of the cross section of the crumpled sheet is examined in the same way. Figure 5 shows the box counting data and the 2D structure factor for the cross section of the crumpled sheets. The horizontal axes are scaled by the 2D radius of gyration

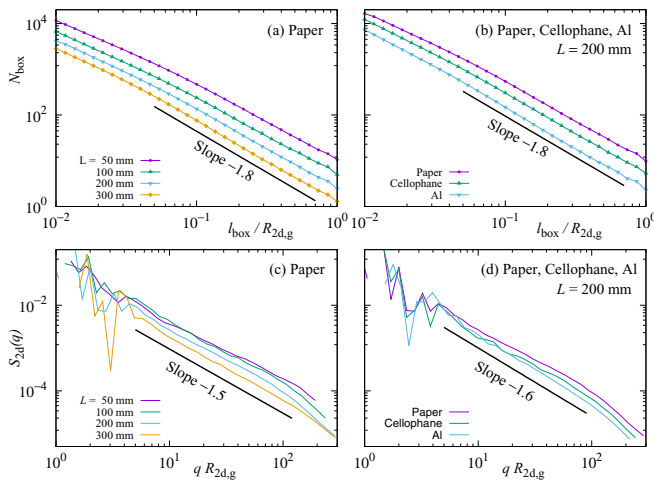


FIG. 5. The box counting numbers N_{box} and the averaged structure factors $S_{2d}(q)$ for the cross sections of crumpled paper sheets, cellophane sheets, and aluminium foils. The box size l_{box} and the wave number q are scaled by the radii of gyration of each structure. N_{box} for different size L (a) and different materials (b) are shifted by the factor 2 to avoid overlapping.

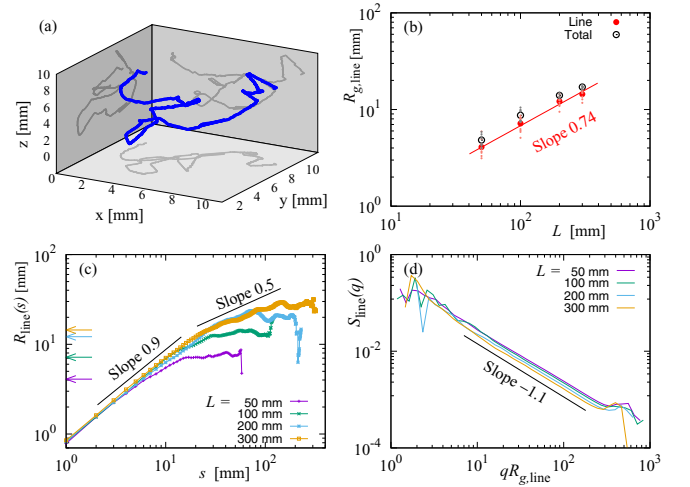


FIG. 6. The structure of a line drawn on a paper. (a) An example of a three-dimensional configuration of a line on a crumpled paper of the size $L = 50$ mm. (b) Radius of gyration vs the paper size L . (c) Averaged root-mean-square displacement at the position s from one of the ends along the line. The arrows indicate the $R_{\text{line},g}$ for each size of the paper. (d) Averaged structure factors $S(q)$. The wave number q is scaled by $R_{g,\text{line}}$ for each size of the paper.

The fractal dimensions $d_{f,\text{cs}}$ for the cross sections are estimated by the box counting method, and we obtain $d_{f,\text{cs}} \approx 1.8$ for the paper of the size $L = 50$ – 300 mm, and $d_{f,\text{cs}} \approx 1.8$ for cellophane and aluminium of the size $L = 200$ mm. The 2D structure factor also shows the power-law behavior

$$S_{2d}(q_{\perp}) \sim q^{-\beta_{\text{cs}}} \quad (28)$$

with the exponent $\beta_{\text{cs}} \approx 1.5$ for the paper and $\beta_{\text{cs}} \approx 1.6$ for the cellophane and the aluminium. Since the self-similarity leads to the relation

$$\beta_{\text{cs}} = d_{f,\text{cs}} = d_f - 1 \quad (29)$$

from Eq. (17), the obtained values for β_{cs} are consistent with the corresponding exponents for the 3D structure.

c. Structure of a line on a crumpled paper: Figure 6(a) shows a configuration of a line on a crumpled paper. The radii of gyration $R_{g,\text{line}}$ for the lines are plotted as a function of the paper size L in Fig. 6(b) along with R_g for the whole structure as have been plotted in Fig. 3(b); the values of $R_{g,\text{line}}$ are somewhat smaller than those of R_g , but the plot is consistent with the power-law behavior with the same exponents as it should be, i.e.,

$$R_{g,\text{line}} \sim L^{\alpha_{\text{line}}}. \quad (30)$$

with $\alpha_{\text{line}} \approx 0.74$. In Fig. 6(c), rms distance $R_{\text{line}}(s)$ defined by Eq. (19) is plotted as a function of s in the logarithmic scale to estimate the Hurst exponent H . The plot shows roughly the power-law behavior

$$R_{\text{line}}(s) \sim s^H \quad (31)$$

with $H \approx 0.9$ for the range $R_{\text{line}}(s) \lesssim R_{g,\text{line}}$, beyond which it saturates and seems to follow the power law with a smaller exponent $H \approx 0.5$, but the range is too small to determine its behavior with confidence. Finally, Fig. 6(d) shows that the 3D

TABLE II. Obtained exponents for the crumpled paper, cellophane, and aluminium foils.

	3D structure			Cross section		Line		
	α	β	d_f	β_{cs}	$d_{f,cs}$	α_{line}	H	β_{line}
Paper ($L = 50\text{--}300$ mm)	0.74	2.5	2.7	1.5	1.8	0.74	0.9	1.1
Cellophane ($L = 200$ mm)	–	2.6	2.8	1.6	1.8	–	–	–
Aluminium foil ($L = 200$ mm)	–	2.6	2.8	1.6	1.8	–	–	–

structure factor for the line $S_{line}(q)$ behaves as

$$S_{line}(q) \sim q^{-\beta_{line}} \quad \text{with } \beta_{line} \approx 1.1. \quad (32)$$

The results by Eqs. (31) and (32) are consistent with the relation (22) but not with the relation (24).

V. DISCUSSIONS

We have estimated several exponents which describe the scaling behaviors of the structure of crumpled sheets; The results are tabulated in Table II. Considering the range of the data points and the data fluctuations, error bars for each exponent would be around ± 0.1 .

As is described in Sec. II, the paper and cellophane samples are scanned 7 days after they are crumpled. This is to avoid the structural relaxation immediately after crumpling and to obtain steady values of measurement. One might wonder if the 7-day waiting time is enough to obtain steady values, especially when logarithmically slow relaxation has been observed up to 3 weeks in similar systems of crumpled thin sheets [16,27,28]. In these works, the slow relaxation is observed in the compaction height under a constant force [27], the diameter of crumpled ball after the folding force is withdrawn [16], and the stress under a constant compression [28]. We have checked if a similar slow relaxation shows any significant effect on the quantities we measure in the present work, but it turns out that the relaxation effects are virtually invisible in the scaling exponents of the structure beyond one hour after crumpling (see the supplemental material).

As we have discussed in Sec. III, the exponents in Table II are related to the two basic exponents: the mass fractal dimension D_M and the fractal dimension d_f . The former represents the scaling behavior among the crumpled balls of the different sheet sizes while the latter describes the self-similarity of the structure of each crumpled sheet. For the paper sheet of the size $L = 50\text{--}300$ mm, the mass fractal dimension estimated from α by Eq. (5) is $D_M \approx 2.7$. The fractal dimension for the internal structure d_f are estimated from the box counting and the structure factor. The structure factor tends to give smaller values for the fractal dimension as has been found also in Ref. [25], but overall data suggest that the fractal dimension is in the range $2.5 \lesssim d_f \lesssim 2.8$. These estimates are consistent with

$$D_M = d_f \quad (33)$$

within the accuracy of our estimate, suggesting that the self-similarity in the structure of each crumpled ball gives rise to the similarity among the balls with different sizes. For the cellophane and the aluminium with the size $L = 200$ mm, the estimated fractal dimension for the structure $2.6 \lesssim d_f \lesssim 2.8$,

which are slightly larger than that for the paper. We do not have data to estimate D_M for the cellophane and the aluminium.

These values for D_M and d_f are somewhat larger than the values obtained for D_M in previous works: 2.51 [9] and $\sim 2.1\text{--}2.5$ [13] for paper, and 2.5 [7,8] and 2.3 [5] for aluminium foil. In these estimates, the external diameter is used for the size of the ball R while in the present work the radius of gyration R_g calculated from the density distribution is used. This may lead to some difference in estimating D_M especially when the data range is not large enough although they should give the same exponent in the limit of the infinite data range. Note that the fractal dimensions obtained in the present work for cellophane and aluminium foil are for the internal structure of each crumpled ball.

The unique piece of information that the micro-CT can provide is the structure of a line drawn of the crumpled paper sheets. The estimated value of the Hurst exponent $H \approx 0.9$ for the short length scale suggests that the line configuration is quite ballistic for the length scale up to R_g , but it eventually approaches the random walk for the longer scale. The value of the Hurst exponent $H \approx 0.9$ is consistent with the relation (22) to the exponent for the structure factor $\beta_{line} \approx 1.1$ but not with the relation (24) to $\alpha_{line} \approx 0.74$ or the mass fractal dimension $D_M \approx 2.7$. In other words, for the line on a crumpled paper, the self-similarity of each line structure in the short length scale is not consistent with the overall scaling on changing the size L in contrast to the case of the whole structure of a crumpled paper, in which case $D_M = d_f$, thus the self-similarity of the internal structure is consistent with the global scaling. The existence of these two regimes for the line structure may come from the layered structure of crumpled sheets. The whole structure of crumpled sheets consists of random folding of a wrinkled sheet, and typical scale of random folding is of order of R_g while wrinkling gives shorter length scale with $H \approx 0.9$.

Before concluding, let us discuss some of the previous works using CT technique. Lin *et al.* [24,25] examined the structure of crumpled aluminium foils by CT. The aluminium foils of different radius $R_0 = 3\text{--}10$ mm are crumpled into the ball with the same final radius $R = 1.5$ mm, i.e., different compaction ratios. They estimate the fractal dimension by the box counting and the correlation dimension as a function of the compaction ratio R/R_0 [25]. Their estimates of the dimensions coincide fairly well with our estimates for the aluminium foil by the box counting and the Fourier transform. They also measured the correlation for the tangent vector and observed the layered structure [24].

Cambou and Menon [23] also used CT to examine the internal structure of crumpled aluminium foils. They obtained

the mass distribution, the distribution of the normal vector and the curvature radii, and found that they are distributed quite uniformly. They also found the layered structure, but again their orientation is distributed uniformly. These uniform distributions might appear to contradict the fractal structure that has been found in the present work as well as earlier studies [13,18,19,25]. They are, however, not contradicting because what they studied are averaged distributions of the quantities. Spatial inhomogeneity of fractal structure varies from a sample to another and thus does not likely show in the averaged distribution.

In the present work, we did not examine the scaling relation with the applied force, Eq. (2). Its exponent δ should represent how the crumpling energy increases as a paper sheet is crumpled into a smaller ball, thus should come from the self-similarity of the internal structure, although we do not know yet how it is related with other exponents.

ACKNOWLEDGMENT

This work is partially supported by JSPS KAKENHI Grant No. JP20K03882.

-
- [1] A. Lobkovsky, S. Gentges, H. Li, D. Morse, and T. A. Witten, *Science* **270**, 1482 (1995).
 - [2] E. Cerda and L. Mahadevan, *Phys. Rev. Lett.* **80**, 2358 (1998).
 - [3] E. Cerda, S. Chaieb, F. Melo, and L. Mahadevan, *Nature (Lond.)* **401**, 46 (1999).
 - [4] T. A. Witten, *Rev. Mod. Phys.* **79**, 643 (2007).
 - [5] A. S. Balankin, I. C. Silva, O. A. Martínez, and O. S. Huerta, *Phys. Rev. E* **75**, 051117 (2007).
 - [6] Y. C. Lin, Y. L. Wang, Y. Liu, and T. M. Hong, *Phys. Rev. Lett.* **101**, 125504 (2008).
 - [7] Y. Kantor, M. Kardar, and D. R. Nelson, *Phys. Rev. Lett.* **57**, 791 (1986).
 - [8] Y. Kantor, M. Kardar, and D. R. Nelson, *Phys. Rev. A* **35**, 3056 (1987).
 - [9] M. A. Gomes, *J. Phys. A: Math. Gen.* **20**, L283 (1987).
 - [10] M. Habibi, M. Adda-Bedia, and D. Bonn, *Soft Matter* **13**, 4029 (2017).
 - [11] S. Deboeuf, E. Katzav, A. Boudaoud, D. Bonn, and M. Adda-Bedia, *Phys. Rev. Lett.* **110**, 104301 (2013).
 - [12] G. A. Vliegthart and G. Gompper, *Nat. Mater.* **5**, 216 (2006).
 - [13] A. S. Balankin, R. Cortes Montes de Oca, and D. S. Ochoa, *Phys. Rev. E* **76**, 032101 (2007).
 - [14] It should be noted that the definition of the applied force F and the radius of crumpled ball R depend on an experimental protocol. Due to the plasticity and the relaxation involved during and after crumpling, there is certain subtleties in what these values really mean, but we will not go into this problem, simply assuming that such ambiguity does not affect the scaling relations we will study in the present work.
 - [15] D. L. Blair and A. Kudrolli, *Phys. Rev. Lett.* **94**, 166107 (2005).
 - [16] A. S. Balankin, O. S. Huerta, R. Cortes Montes de Oca, D. S. Ochoa, J. Martínez Trinidad, and M. A. Mendoza, *Phys. Rev. E* **74**, 061602 (2006).
 - [17] C. A. Andresen, A. Hansen, and J. Schmittbuhl, *Phys. Rev. E* **76**, 026108 (2007).
 - [18] A. S. Balankin, A. Horta Rangel, G. García Pérez, F. Gayosso Martinez, H. Sanchez Chavez, and C. L. Martínez-González, *Phys. Rev. E* **87**, 052806 (2013).
 - [19] A. S. Balankin, D. S. Ochoa, I. A. Miguel, J. P. Ortiz, and M. Angel Martinez Cruz, *Phys. Rev. E* **81**, 061126 (2010).
 - [20] T. Tallinen, J. A. Åström, and J. Timonen, *Phys. Rev. Lett.* **101**, 106101 (2008).
 - [21] T. Tallinen, J. A. Åström, and J. Timonen, *Nat. Mater.* **8**, 25 (2009).
 - [22] S.-F. Liou, C.-C. Lo, M.-H. Chou, P.-Y. Hsiao, and T.-M. Hong, *Phys. Rev. E* **89**, 022404 (2014).
 - [23] A. D. Cambou and N. Menon, *Proc. Natl. Acad. Sci. USA* **108**, 14741 (2011).
 - [24] Y.-C. Lin, J.-M. Sun, J.-H. Hsiao, Y. Hwu, C. L. Wang, and T.-M. Hong, *Phys. Rev. Lett.* **103**, 263902 (2009).
 - [25] Y.-C. Lin, J.-M. Sun, H. W. Yang, Y. Hwu, C. L. Wang, and T.-M. Hong, *Phys. Rev. E* **80**, 066114 (2009).
 - [26] See Supplemental Material at <http://link.aps.org/supplemental/10.1103/PhysRevE.104.025005> for the relaxation effects during the 7-day waiting time in the sample preparation.
 - [27] K. Matan, R. B. Williams, T. A. Witten, and S. R. Nagel, *Phys. Rev. Lett.* **88**, 076101 (2002).
 - [28] Y. Lahini, O. Gottesman, A. Amir, and S. M. Rubinstein, *Phys. Rev. Lett.* **118**, 085501 (2017).